Mesoblends of Polyether Block Copolymers with Poly(ethylene glycol)

Nikunj P. Patel[†] and Richard J. Spontak*[,†,‡]

Departments of Chemical Engineering and Materials Science & Engineering, North Carolina State University, Raleigh, North Carolina 27695

Received October 28, 2003; Revised Manuscript Received December 9, 2003

ABSTRACT: Mesoblends are conveniently generated by sorbing a parent homopolymer into a microphase-separated triblock or higher-order multiblock copolymer swollen by a block-selective solvent. These nonequilibrium systems afford a viable route by which to produce, in systematic fashion, novel copolymer/homopolymer blends as well as explore homopolymer transport and solubility within a molecularly confined polymer environment. In the present work, we have imbibed poly(ethylene glycol) (PEG) differing in molecular weight into a model poly(styrene-*b*-ethylene oxide-*b*-styrene) (SEOS) triblock copolymer and a commercial poly(amide-*b*-ethylene glycol) (AEG) multiblock copolymer. Solvent quality and solution concentration are found to have a profound effect on PEG solubility in both copolymers, whereas PEG molecular weight over the range 100−4600 is generally less influential. Transmission electron microscopy reveals the spatial distribution of amorphous PEG within the SEOS copolymer matrix, and complementary differential scanning calorimetry establishes the role of added PEG on the thermal behavior of the copolymer midblock. Incorporation of PEG into the AEG copolymer serves to improve the CO_2/H_2 selectivity of this material at ambient temperature and low pressure.

Introduction

The current generation of polymeric materials is being designed to meet the needs of contemporary technologies by employing multicomponent systems in which a homopolymer or copolymer is controllably modified through the addition of (i) one or more macromolecules to form a blend/alloy[1−3] or (ii) an inorganic species to form a nanocomposite.[4−6] Such systems exhibit the multifunctionality required for either improved processing or ultimate application and permit tremendous versatility in terms of materials design. In this work, we consider the modification of microphase-separated block copolymers through the incorporation of a parent homopolymer. Block copolymers, macromolecules composed of long, contiguous sequences arranged in a variety of architectures, can microphase-order if the sequences are sufficiently incompatible.[7,8] For linear molecules, the thermodynamic incompatibility is conveniently expressed by χN, where χ denotes the temperature-dependent Flory−Huggins interaction parameter and N is the number of statistical units along the copolymer backbone.[9] Microphase-ordering promotes self-organization of binary block copolymer molecules composed of A and B units into several periodic nanostructures predominantly regulated by composition and described as A(B) spheres positioned on a body-centered-cubic lattice in a B(A) matrix, hexagonally packed A(B) cylinders in a B(A) matrix, bicontinuous channels, or alternating lamellae. While only binary (AB) copolymers are explicitly considered here, a greatly expanded list of accessible morphologies is available with ternary (ABC) block copolymers.[8,10] Higher-order multiblock copolymers may, however, organize into nanoscale domains without long-range (periodic) order due to greater block connectivity and the accompanying propensity for kinetic entrapment.[11]

In neat block copolymers, production of a specific nanostructure for a given application requires tailored molecular synthesis, which can be pragmatically undesirable. An alternative approach to nanostructure design in block copolymers involves blending a copolymer capable of microphase-ordering with a parent homopolymer[12−14] or a second copolymer.[15−18] Under the right set of composition and molecular weight conditions,[19] the two macromolecules remain miscible and form a single new morphology, which may be unobtainable in the neat copolymer alone.[20] Traditional efforts designed to introduce a parent homopolymer into a microphase-ordered block copolymer via "equilibrium" routes (e.g., codissolution in and cocasting from a common solvent) have established that, at low concentrations, the homopolymer molecules swell the host microphases of the copolymer. At higher concentrations, an added homopolymer that adequately interpenetrates (*wets*) the brush of the compatible copolymer block can alter interfacial curvature and thereby induce a morphological transition. The nonequilibrium analogues to such blends are block copolymer/homopolymer *mesoblends*, in which a parent homopolymer is sorbed into a microphase-separated block copolymer via a selective carrier solvent (see Figure 1). This idea originates from the concept of block copolymer/solvent *mesogels* introduced by Zhulina and Halperin[21] and later verified by King et al.[22] Our recent studies[23,24] of block copolymer/homopolymer mesoblends have explored lamellar poly(styrene-*b*-isoprene-*b*-styrene) (SIS) copolymers to which polyisoprene (PI) is imbibed from *n*-hexane. Results from those studies indicate that (i) PI uptake is sensitive to homopolymer molecular weight and solution concentration and (ii) the resultant mesoblend morphologies differ considerably from those realized by equilibrium routes.

Previous endeavors to elucidate homopolymer sorption and accompanying structure−property development in block copolymer/homopolymer mesoblends have been complicated by the use of a carrier solvent that has low, but nonnegligible, solubility in the microphases formed

[†] Department of Chemical Engineering.
[‡] Department of Materials Science & Engineering.
* To whom correspondence should be addressed: e-mail rich_spontak@ncsu.edu.

10.1021/ma0356257 CCC: $27.50
Published on Web 01/27/2004

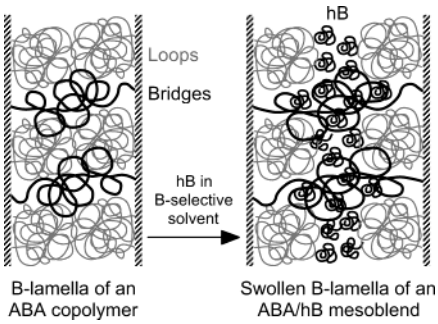

Figure 1. Schematic illustration of the general approach to preparing a block copolymer/homopolymer mesoblend with a microphase-ordered ABA triblock copolymer. The copolymer molecules spontaneously order into A and B lamellae, the latter of which are composed of looped and bridged copolymer midblocks. Immersion of the copolymer into a B-selective solvent containing dissolved homopolymer B (hB) results in sorption of hB molecules into, and subsequent swelling of, the B lamellae. If the carrier solvent is a nonsolvent for the A lamellae, they are expected to remain intact despite the stress buildup due to copolymer swelling.

by the incompatible styrenic blocks. Such limited solubility sufficiently softens the glassy lamellae to permit molecular rearrangement into nonlamellar morphologies due to the high osmotic pressure induced by the hexane-swollen I microphases. In the present work, this complication is alleviated by employing polyether-containing block copolymers to which poly(ethylene glycol) (PEG) is imbibed into the copolymers from highly polar solvents (e.g., water and short-chain alcohols), which do not permit the hard (mechanically stabilizing) microphases of the copolymers to rearrange to a discernible extent. This is the same general strategy adopted by Wiesner and co-workers[25] in their preparation of nanoscale objects from water-soluble ceramic precursors sorbed into polyether-containing block copolymer templates. Another reason for examining mesoblends of these particular copolymer−homopolymer pairs is the ongoing interest in developing highly CO_2-selective membranes to be used in gas-separation applications.[26] Bondar et al.[27] and Kim et al.[28] have previously demonstrated that randomly coupled multiblock copolymers composed of polyamide hard blocks and PEG soft blocks exhibit very high CO_2/H_2 selectivity (α), which is defined as

$$\alpha \equiv P_{CO_2}/P_{H_2} \tag{1}$$

If molecular transport is accurately described by a solution-diffusion process,[29] the permeability of each gas through the membrane (P_i, where i is either CO_2 or H_2) is given by the following:

$$P_i = D_i S_i \tag{2}$$

Here, D_i and S_i denote the diffusivity and solubility of penetrant species i in the membrane. We have shown[30] that α of a polyether block copolymer can be improved substantially upon addition of PEG via codissolution/casting and now seek to discern whether comparable property enhancement can be likewise achieved with block copolymer/homopolymer mesoblends.

Experimental Section

Materials. A model poly(styrene-*b*-ethylene oxide-*b*-styrene) (SEOS) triblock copolymer was obtained in powder form from Polymer Source, Inc. (Dorval, Canada). According to ^{1}H NMR and GPC analyses conducted by the manufacturer, the composition, number-average molecular weight, and polydispersity of the copolymer were 57 wt % S, 69 000, and 1.03, respectively. A commercial poly(amide-*b*-ethylene glycol) (AEG) multiblock copolymer known as PEBAX 1074 was supplied by Elf Atochem (Philadelphia, PA) in pellet form. The hard amide block is composed of nylon-12, poly[imino(1-oxododecamethylene)], and accounts for 45 wt % of the copolymer, according to the manufacturer. While information regarding molecular weight and average block lengths in this randomly coupled multiblock copolymer is unavailable, previous studies have reported[27] that the amide block is semicrystalline and that the polyether blocks are sufficiently short to remain liquid. Several PEG oligomers with molecular weights ranging from 100 to 4600 were purchased from Aldrich (Milwaukee, WI) and used as-received. Each oligomer is hereafter designated as PEG_M, where the subscript M denotes the molecular weight. With the exception of the highest-molecular-weight grade (PEG_{4600}, which exists as a semicrystalline powder), all the remaining PEG oligomers were received in liquid form. Chloroform, methanol, ethanol, and 1-butanol were likewise purchased from Aldrich and used without further purification.

Methods. Bulk films of the SEOS copolymer were produced from 5 to 10% (w/v) copolymer solutions in chloroform. After ample dissolution time, the solutions were cast in Teflon molds, and the solvent was permitted to evaporate over the course of 2 weeks at ambient temperature. Resultant films measuring 100−300 μm in thickness were annealed for 24 h at 100 °C to remove residual solvent and promote nanostructural refinement prior to removal from the mold in liquid nitrogen. The AEG copolymer possesses greater solvent resistance and was consequently dissolved in 1-butanol at 80 °C to form a 4% solution. To avoid premature precipitation of the copolymer during film formation, the solution was cast and the solvent was evaporated over the course of 2 weeks at the dissolution temperature. The AEG films produced in this fashion measured 50−200 μm thick and were subsequently annealed for 24 h at 60 °C for the same purposes as above.

In the sorption tests, dried copolymer films were cut into sheets measuring ca. 0.5 cm × 0.5 cm and weighed. Each PEG was dissolved at a predetermined concentration in a specific solvent. Copolymer sheets were immersed in each chosen solution within an isolated beaker. After a given sorption time, each film was removed from the solution, and excess solvent on the film surface was blotted with filter paper. Swollen films were initially dried under ambient conditions, followed by vacuum-drying at 60 °C overnight to remove residual solvent. The mass of sorbed PEG was determined directly from gravimetric analysis. Copolymer films were also suspended in pure solvent and measured in the same fashion to ensure that no solvent remained in the film after vacuum-drying and that the results were free of solvent artifacts. Any measurable increase in weight after vacuum-drying was attributed solely to sorbed PEG.

The location of the sorbed PEG within the SEOS copolymer matrix was determined by transmission electron microscopy (TEM). Films of the neat copolymer and several of its PEG-modified mesoblends were sectioned at −100 °C in a Leica Ultracut-S cryoultramicrotome to yield ∼100 nm specimens, which were subsequently subjected to the vapor of a 4% OsO_4-(aq) solution for 90 min at ambient temperature. The stained specimens were imaged with a Zeiss EM902 electron spectroscopic microscope operated at 80 kV and energy-loss (ΔE) settings of 60−110 eV. Negative plates were scanned at 1000 dpi and enlarged for analysis and presentation purposes. The thermal characteristics of the pure and PEG-swollen SEOS block copolymer were measured by differential scanning calorimetry (DSC) with a Perkin-Elmer DSC-7 unit. Data were collected under a nitrogen blanket in a heat−cool−heat cycle to ascertain the effect of thermal treatment on mesoblend stability. Heating and cooling rates were held constant at 20 and −20 °C/min, respectively. The normal melting (T_m) and crystallization (T_f) temperatures reported herein correspond to peak temperatures, and the degree of crystallinity (X_c) for

the neat SEOS copolymer is calculated from

$$X_c = \Delta H_m/(W_{EO}\Delta H_m°) \quad (3)$$

where ΔH_m is the latent heat of melting approximated by the area under the melting endotherm, $\Delta H_m°$ is the latent heat of melting for 100% crystalline poly(ethylene oxide) (186.188 J/g, as reported elsewhere[31]), and W_{EO} is the weight fraction of the crystallizable midblock of the SEOS copolymer. In the SEOS/PEG mesoblends, W_{EO} is replaced by the quantity $[W_{EO}(1 - W_{PEG}) + W_{PEG}]$, where W_{PEG} refers to the mass fraction of sorbed PEG, since both contributing polyether constituents are capable of crystallizing.

Pure-gas permeation properties of the neat AEG copolymer and its PEG mesoblends were measured by the constant-volume/variable-pressure method.[32] The setup used here consisted of a downstream vessel of known volume (V), a permeation cell containing a polymer film, and an upstream vessel maintained at a designated temperature. Vacuum was pulled on both sides of the film before exposing the upstream side to a desired gas pressure (p_2). As the gas permeated through the film, the pressure on the downstream side was monitored until the pressure increase rate (dp/dt) remained constant. The permeability of the gas was determined from

$$P_i = (Vl/ARTp_2)(dp/dt) \quad (4)$$

where l is the film thickness, A is the exposed film area, R is the gas constant, and T denotes absolute temperature. In all the permeation tests discussed here, the highest downstream pressure was 0.007 atm, in which case p_2 effectively corresponds to the transmembrane pressure.

Results and Discussion

Mesoblends Derived from the SEOS Triblock Copolymer. Sorption of PEG into the SEOS copolymer is complicated by two considerations. The first obstacle in this endeavor is the inherent crystallinity of the relatively high-molecular-weight EO midblock of the copolymer. The value of T_m associated with the EO midblock is, according to DSC analysis,[30] 50 °C, which, due to molecular-level confinement within a microphase-separated (lamellar) morphology, deviates substantially from the normal melting point of pure poly(ethylene oxide) (PEO) of comparable molecular weight (72 °C, according to ref 31). Chen et al.[33] have reported that such confinement effects not only tend to reduce T_m in EO-containing block copolymers but also become more pronounced as the EO block is more highly constrained in dispersed morphologies (i.e., cylinders and spheres). The complication afforded by impermeable EO crystals in the present work is readily overcome by sorbing PEG into the copolymer at a temperature that is higher than T_m. In this same vein, an upper sorption temperature set by the styrenic blocks of the copolymer likewise exists. Since the hard (glassy) blocks must remain relatively impervious to solvent-induced swelling and alteration so that the copolymer remains microphase-ordered during PEG sorption, the sorption temperature cannot exceed the glass transition temperature (T_g) of the styrenic block, which is measured[30] to be 92 °C in the neat copolymer. Thus, to preclude the possibility of softening the glassy styrenic microdomains during PEG sorption into amorphous EO-rich microdomains, the sorption temperature is held constant at 60 °C unless otherwise specified.

The second challenge to be considered is the choice of carrier solvent from which PEG sorption into the copolymer will take place. While PEG with a solubility parameter (δ) ranging from 19.2 to 30.6 MPa$^{1/2}$ depending on molecular weight (according to group-contribution methods[34]) is soluble in a wide variety of common solvents (including water), the solvent must be selected so that it does not interact substantially with the ordered styrenic microdomains (with $\delta = 18.7$ MPa$^{1/2}$ from ref 35) for the same reasons discussed above. Roberge et al.[23] have shown that even low solvent solubility within the styrenic microdomains is sufficient to permit spectacular morphological changes within the ordered copolymer. Water, assigned[35] $\delta = 47.9$ MPa$^{1/2}$, is therefore the obvious choice for PEG sorption, since it constitutes a nonsolvent for polystyrene. As the uptake kinetic data presented in Figure 2a demonstrate, however, use of water results in little sorption of PEG_{400} into the copolymer. In this and subsequent figures, each datum point represents a fresh sample. According to Figure 2a, W_{PEG} is only 0.06 after ~100 h of immersion time (t) in a 20% w/v PEG_{400} solution. This problem arises due to the inherent hydrophobicity of the styrenic microdomains and can be overcome by using a polar organic solvent, such as a short-chain alcohol. As the data displayed in Figure 2a attest, use of ethanol ($\delta = 26.0$ MPa$^{1/2}$ from ref 35) instead of water as the carrier solvent promotes a substantial increase in sorbed PEG_{400} ($W_{PEG} = 0.58$ at $t \sim 100$ h) under identical temperature and solution concentration conditions. At long immersion times in both solvents, the concentration of sorbed PEG becomes constant and corresponds to the solubility (S) under the conditions identified.

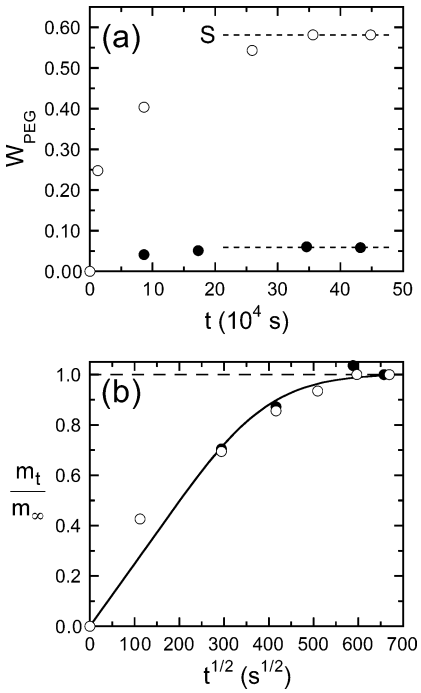

Figure 2. Mass uptake kinetics of PEG_{400} in the SEOS triblock copolymer after immersion in a 20% w/v solutions in ethanol (○) and water (●) at 60 °C. In (a), the fraction of PEG_{400} in the resultant mesoblend (W_{PEG}) is displayed as a function of time (t), and the equilibrium solubility (S, dashed horizontal lines) is defined. In (b), the mass of sorbed PEG_{400} at time t relative to that at long time is shown as a function of $t^{1/2}$, and the regressed curve corresponds to eq 5 in the text.

The data presented in Figure 2a are replotted in Figure 2b in the more familiar form of m_t/m_∞, where m_t denotes the mass uptake of PEG sorbed at time t and m_∞ is the mass uptake at long t (at the solubility limit), as a function of $t^{1/2}$ to confirm that the mechanism of molecular mobility is Fickian diffusion. Moreover, the

PEG_{400} uptake data collected from both solvents are observed to superimpose, indicating that, although the two solvents promote drastically different PEG_{400} solubilities (see Figure 2a), the mobility of PEG_{400} molecules into the solvent-swollen copolymer matrices is essentially independent of carrier solvent. Values of an effective diffusion coefficient (D_{eff}) can be extracted from the data provided in Figure 2b using a variety of protocols (most of which rely on the initial slope of the sorption curve).[36] For consistency with our previous study,[24] we elect to use the Balik[37] model for fitting the entire sorption curve with a single expression:

$$\frac{m_t}{m_\infty} = \phi(x)\, f(x) + [1 - \phi(x)]g(x) \tag{5}$$

where $x = D_{eff}t/L^2$ and L is the thickness of the film. The short- and long-time contributions to eq 5 are given by

$$f(x) = 4(x/\pi)^{1/2} \tag{6a}$$

and

$$g(x) = 1 - (8/\pi^2)e^{-\pi^2/x} \tag{6b}$$

respectively, and the weighting factor $\phi(x)$ is derived on the basis of the Fermi function, namely

$$\phi(x) = (1 + e^{(x-a)/b})^{-1} \tag{7}$$

Here, the parameters a and b are set[37] equal to 0.05326 and 0.001, respectively. The value of D_{eff} determined by fitting eq 5 to all the data in Figure 2b is $(1.1 \pm 0.1) \times 10^{-9}$ cm^2/s irrespective of solvent. For comparison, the value of D_{eff} deduced[24] for PI sorbed into a lamellar SIS copolymer swollen by *n*-hexane is about an order of magnitude larger, $(3.3 \pm 0.7) \times 10^{-8}$ cm^2/s (independent of midblock molecular weight), which indicates that the PI has greater mobility in the swollen SIS copolymer than PEG_{400} in the SEOS copolymer despite its larger size ($M_{PI} = 7500$) and a pendant methyl group in its repeat unit. Possible explanations for this disparity include a more tortuous (less interconnected) lamellar morphology or the presence of physical obstacles (e.g., incompletely dissolved EO crystals) in the SEOS copolymer matrix. Alternatively, since *n*-hexane has been reported[23] to modify the inherent morphology of the SIS copolymer by introducing perforations into the styrenic lamellae, it is conceivable that additional diffusive pathways may have become accessible through which the PI molecules could diffuse.

The data displayed in Figure 2 have been collected from solutions in which the concentration of PEG_{400} was maintained at 20% w/v. Figure 3 shows the effect of solution concentration (C) in both water and ethanol on PEG_{400} solubility (S) in the SEOS copolymer after 100 h at 60 °C. Increasing C under isothermal conditions renders a larger chemical potential difference, which ultimately leads to enhanced solubility, as Figure 3 confirms. In water, S increases almost linearly with increasing C up to 70% w/v PEG_{400}. A qualitatively similar trend has been reported by Stevens et al.[24] for PI in swollen SIS copolymers differing in midblock molecular weight. According to Figure 3, the slope $(\partial S/\partial C)_T$ ascertained for PEG_{400} sorbed from water into the SEOS copolymer is about 0.31, which is much lower in magnitude than comparable slopes measured for PI

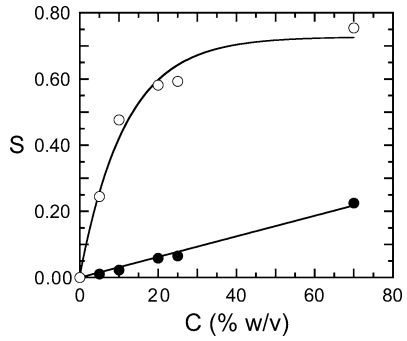

Figure 3. Effect of solution concentration (C) on PEG_{400} solubility (S) in the SEOS copolymer swollen by ethanol (○) and water (●) for 100 h at 60 °C. The solid lines serve as guides for the eye.

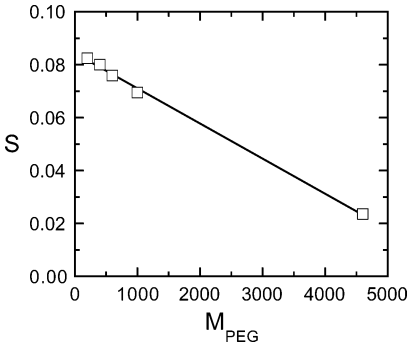

Figure 4. Dependence of PEG solubility in the SEOS copolymer on PEG molecular weight (M_{PEG}) in 25% w/v solutions in methanol at 23 °C. The solid line is a linear regression of the data.

sorbed from *n*-hexane into SIS copolymers (3.9−9.0, depending on midblock molecular weight). In marked contrast, the solubility of PEG_{400} sorbed from ethanol is observed to increase abruptly at low C and reach a limiting value in the range 0.7−0.8 at high C. Thus, use of ethanol as the carrier solvent greatly increases the propensity for PEG_{400} molecules to enter the swollen EO lamellae of the SEOS copolymer relative to water at a fixed solution concentration. The explicit effect of solvent quality on S is discussed further in a later section. Another design issue to be considered is the molecular weight of the sorbed PEG (M_{PEG}). In Figure 4, S is presented as a function of M_{PEG} after immersion of the SEOS copolymer for 24 h in a 25% w/v PEG/methanol solution ($\delta = 29.6$ MPa$^{1/2}$ for methanol[35]) maintained at ambient temperature. Note that the temperature is below the melting point of the EO block, which strongly suggests that residual EO crystals reside in the copolymer matrix. This variation in temperature (and, to a much lesser extent, solvent) provides a clear indication of how the presence of EO crystals negatively impacts the extent to which PEG can be sorbed. At 60 °C, for instance, the solubility of PEG_{400} in the SEOS copolymer swollen under the same solvent/concentration/time conditions in Figure 4 is about 0.37, which is considerably larger than the ∼0.08 measured at 23 °C. In addition, the data shown in this figure provide evidence that an increase in M_{PEG} promotes an almost linear decrease in S, which is contrary to the $S \sim M_{PI}^{-1/2}$ dependence reported[23] for the sorption of PI varying in molecular weight into a SIS copolymer swollen by *n*-hexane. While such a reduction in S is to be qualitatively expected a priori on the basis of the increased incompatibility and entropic penalty (brush dewetting) encountered with

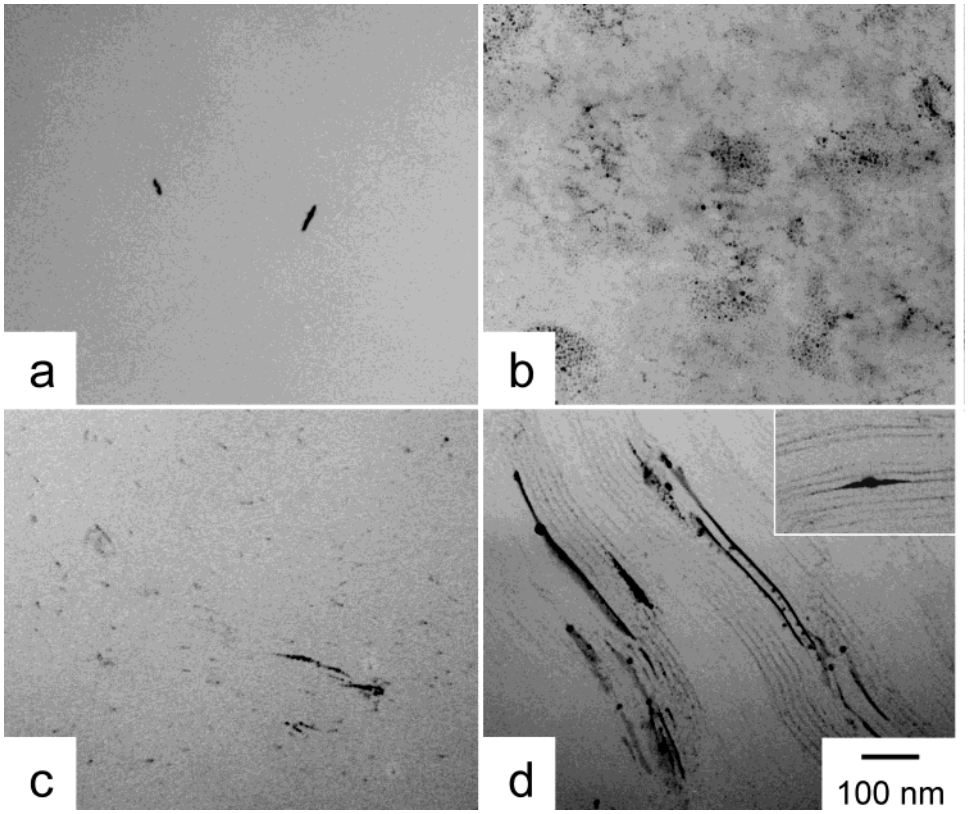

Figure 5. Series of TEM images obtained from (a) the neat SEOS triblock copolymer and three SEOS/PEG mesoblends composed of (b) PEG_{4600} from ethanol, (c) PEG_{400} from water, and (d) PEG_{400} from ethanol. Mesoblend preparation conditions include a 100 h immersion time at 60 °C in 25% w/v solutions. The electron-opaque (dark) features identify amorphous PEG that has been selectively stained by OsO_4. The inset in (d) is at the same magnification as the primary images.

increasing M_{PEG}, the difference in the dependence of S on M_{PEG} is not so obvious. We return later to discuss these relationships.

Factors governing the sorption of PEG into a solvent-swollen SEOS copolymer have thus far been identified and discussed. In this section, we explore the effect of sorbed PEG on the morphology and thermal properties of SEOS/PEG mesoblends. The TEM images displayed in Figure 5 have been acquired from the neat SEOS copolymer (Figure 5a) as well as the copolymer immersed at 60 °C for 100 h in 25% w/v solutions of PEG_{4600} in ethanol (Figure 5b), PEG_{400} in water (Figure 5c), and PEG_{400} in ethanol (Figure 5d). In all cases, only the amorphous PEG present is stained by the OsO_4(aq) treatment described in the Experimental Section and consequently appears electron-opaque (dark). In Figure 5a, the two features visible in the image correspond to contaminants used for focusing purposes. It is interesting to note that none of the EO units within the copolymer are stained and, by inference, amorphous. According to thermal calorimetry, the EO microdomains of this copolymer are only about 22% crystalline, which appears sufficiently high to preclude staining of the amorphous segments of the EO blocks to any discernible extent. The image in Figure 5b, on the other hand, clearly confirms the presence of amorphous (stained) PEG throughout the mesoblend. Faint features and the discrete black dots, attributed to amorphous PEG residing at the surface of the microtomed section and measuring ca. 3−9 nm in diameter, show no evidence of spatial regularity, which suggests that sorption of PEG_{4600} into the copolymer may not be uniform throughout the lamellar matrix. The effect of added PEG_{4600} on mesoblend crystallinity will be addressed further in a subsequent section.

Sorption of PEG_{400} into the SEOS copolymer from water and ethanol solutions (Figure 5, c and d, respectively) results in very different mesoblend morphologies. The image presented in Figure 5c shows the presence of numerous elongated "dispersions" measuring as long as ∼40 nm and as wide as ∼4 nm as well as several large features measuring more than 80 nm long and about 8 nm wide. Close examination of this and related images reveals that many of these "dispersions" are often oriented along a common direction. This spatial distribution strongly suggests that the amorphous PEG_{400} molecules sorb into the EO lamellae and, due to the low level of sorbed PEG_{400} ($S = 0.07$ from Figure 3), form discrete, amorphous aggregates within the lamellae upon crystallization of the EO blocks. In a few instances, these isolated aggregates appear to be sufficiently numerous to converge into continuous amorphous channels in the otherwise semicrystalline EO lamellae. By changing the solvent to ethanol and thereby increasing the solubility of PEG_{400} within the swollen SEOS copolymer ($S = 0.59$), this tendency is markedly improved, resulting in numerous lamellae that exhibit evidence of stained PEG. The thickness and period of these long, amorphous channels, which consist of pure PEG_{400} or, more likely, a mixture of PEG_{400} and noncrystalline EO segments, measure 2.8 ± 0.6 and 13.7 ± 0.6 nm, respectively. In light of these dimensions, it is comforting to recognize that the unperturbed gyration diameter of a PEO coil with $M = 400$ is estimated[34] to be 1.4 ± 0.2 nm. Moreover, the period extracted from Figure 5d is slightly larger than that discerned from

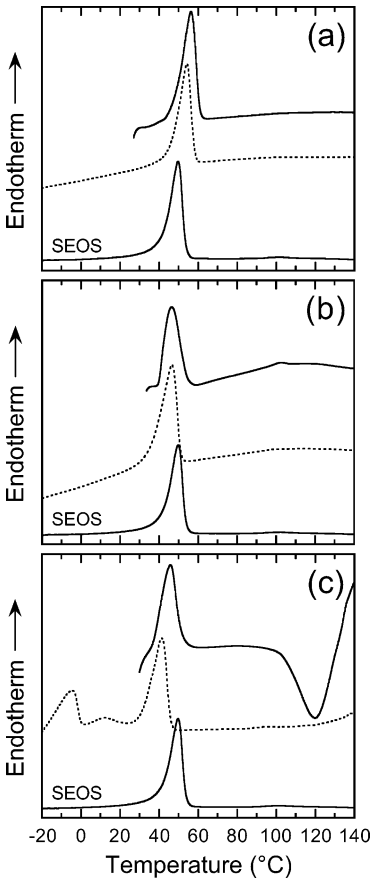

Figure 6. DSC thermograms of the three mesoblends described in Figure 5: (a) PEG_{4600} from ethanol, (b) PEG_{400} from water, and (c) PEG_{400} from ethanol. Shown here are the first-heat cycle (solid line) and the second-heat cycle (dashed line). Included for comparison in each part is the thermogram of the neat SEOS copolymer to facilitate direct comparison.

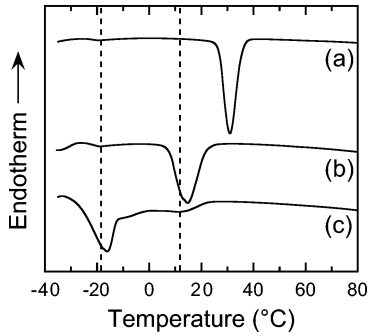

Figure 7. DSC thermograms showing the first cooling cycle of the three mesoblends discussed with regard to Figure 6: (a) PEG_{4600} from ethanol, (b) PEG_{400} from water, and (c) PEG_{400} from ethanol. The vertical dashed lines identify the temperatures of relatively weak exothermic transitions to allow comparison.

the neat copolymer,[38] which confirms that the EO lamellae are swollen due to the presence of sorbed PEG_{400}. The intensely dark features are again attributed to amorphous PEG lying on (or, in the case of PEG_{400}, possibly migrating to) the surface of the microtomed section.

The thermal characteristics of the three mesoblends featured in Figure 5 are provided in Figures 6 and 7. In Figure 6, first- and second-heat cycles of the mesoblends prepared with PEG_{4600}/ethanol (Figure 6a), PEG_{400}/water (Figure 6b), and PEG_{400}/ethanol (Figure 6c) are compared with the first-heat cycle of the neat SEOS copolymer. Initial sorption of PEG_{4600} into the copolymer induces a shift in T_m from 50 to 56 °C. During the second heating cycle, the mesoblend is closer to an "equilibrium" blend in which nonequilibrium characteristics have been thermally erased to a relatively large extent. In this case, T_m of the SEOS/PEG_{4600} blend is only slightly lower than T_m of the initial mesoblend (54 °C), and the corresponding crystallinity of the blend calculated from eq 3 is about 77% higher than that of the neat copolymer. Corresponding values of ΔH_m and X_c measured from each of the systems and heating cycles portrayed in Figure 6 are listed in Table 1. The thermograms provided in Figure 6b show that the addition of PEG_{400} from water has an insignificant effect on T_m and X_c during the first- and second-heat cycles, which is consistent with the very low level of PEG_{400} sorbed from water. Several intriguing features are evident, however, in the SEOS/PEG_{400} mesoblends prepared from ethanol. The first-heat cycle indicates that T_m is lowered slightly, but X_c is reduced considerably (see Table 1), upon incorporation of PEG_{400}. While these characteristics are interesting in their own right, a second feature absent in thermograms of the other two mesoblends is a large exothermic process that begins at the T_g of the styrenic blocks comprising the copolymer. This process is attributed to the immense stress placed on the glassy lamellae by the presence of imbibed PEG_{400} molecules. At a comparable PEG_{400} concentration in equilibrium SEOS/PEG_{400} blends, the morphology transforms from alternating lamellar to a continuous polyether matrix, according to thermal calorimetry and permeation measurements.[30]

Thus, we propose that the exothermic process visible in the first-heat thermogram of Figure 6c reflects the release of stress built up in the mesoblend (due to constrained swelling) by morphological alteration once the styrenic microdomains soften and become pliable at and above their T_g. This hypothesis is consistent with the second-heat cycle in Figure 6c, from which evidence of residual PEG/EO segregation can be gleaned. The first endotherm in the vicinity of −4 °C can most likely be assigned to PEG_{400} (which possesses a softening point of −6 °C, according to the manufacturer), whereas the second, broad endotherm centered at about 12 °C is attributed to cocrystallization of the PEG_{400} molecules and the EO blocks of the copolymer. The third, sharp endotherm corresponds to crystallization of the EO blocks and is shifted to lower temperature (41 °C) due to PEG_{400} dilution. Similar results are apparent in the cooling curves displayed in Figure 7 for all three mesoblends. In the case of the SEOS/PEG_{4600} system, the principal crystallization exotherm lies at 31 °C,

Table 1. Thermal Properties of the SEOS Copolymer and Its Mesoblends with PEG[a]

system	W_{PEG}	heating cycle	ΔH_m (J/g)	X_c
SEOS	0.00	1	17.2	0.21
		2	17.7	0.22
SEOS/PEG_{4600}/ethanol	0.18	1	35.5	0.36
		2	38.2	0.39
SEOS/PEG_{400}/water	0.07	1	16.9	0.19
		2	17.9	0.21
SEOS/PEG_{400}/ethanol	0.59	1	13.6	0.10
		2	9.6	0.07

[a] Determined from the DSC thermograms displayed in Figure 6.

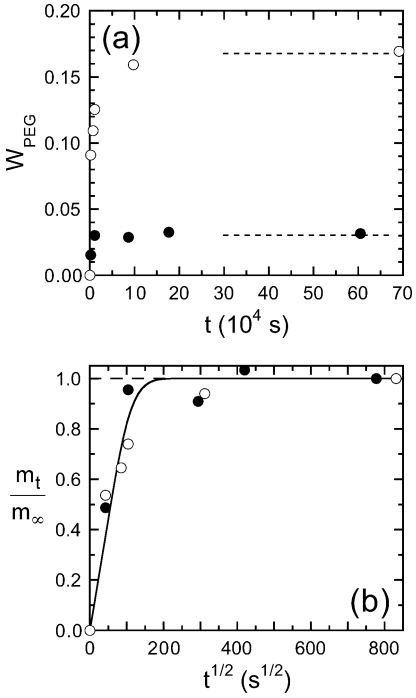

Figure 8. Mass uptake kinetics of PEG_{400} in the AEG multiblock copolymer at 23 °C after immersion in ethanol solutions at two different concentrations (in % w/v PEG_{400}): 20 (●) and 60 (○). The format of parts (a) and (b) is identical to that described in Figure 2 regarding PEG_{400} sorption into the SEOS triblock copolymer.

whereas a significantly smaller crystallization event occurs at about −19 °C. Upon sorption of PEG_{400} from water, the resultant mesoblend exhibits a reduced primary crystallization point (15 °C) and a slightly more pronounced peak in the vicinity of −19 °C. Substitution of ethanol for water as the carrier solvent for PEG_{400} yields a broad crystallization exotherm at ∼11 °C, a shoulder at −7 °C, and a principal peak at −16 °C. Recall that, while the two mesoblends prepared from PEG_{4600}/ethanol and PEG_{400}/water display only a single melting peak upon reheating, the one imbibed with PEG_{400} from ethanol similarly exhibits several melting events, indicative of PEG_{400} segregation within the EO-rich microdomains. This result is consistent with the amorphous PEG channels visible in Figure 5d.

Mesoblends Derived from the AEG Multiblock Copolymer. Unlike the SEOS copolymer, the AEG copolymer consists of semicrystalline hard (nylon-12) blocks and liquid soft (PEG) blocks arranged in a randomly coupled multiblock architecture. While the polyamide block is capable of imbibing polar solvents due to its hydrogen-bonding nature, the moisture content in nylon-12 immersed in liquid water at 23 °C is reported[39] to be only 1.5%. Thus, it is sensible to expect that the polyamide blocks and their corresponding microdomain structure will be virtually unaffected by the carrier solvent or sorbed PEG during AEG/PEG mesoblend preparation. Since the PEG blocks are intrinsically molten at ambient temperature (T_m is measured[27] to be 11 °C), it is unnecessary to heat the specimens to promote sorption of PEG from solution. Mass uptake curves obtained at 23 °C for PEG_{400} sorbed into the AEG copolymer from 20 and 60% w/v solutions in ethanol are displayed for comparison in Figure 8. As with the SEOS/PEG_{400} mesoblends (see Figure 3), an increase in solution concentration (C) is accompanied

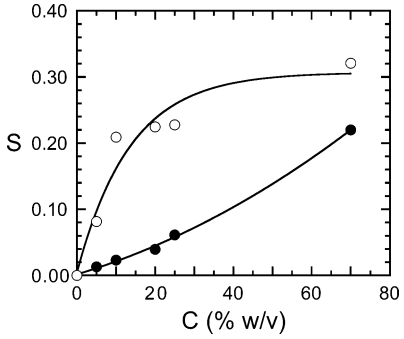

Figure 9. Effect of solution concentration on PEG_{400} solubility in the AEG copolymer swollen by ethanol (○) and water (●) for 100 h at 60 °C. The solid lines are guides for the eye.

by an increase in PEG_{400} solubility (S) according to Figure 8a. Normalization of the mass uptake curves in the form required for analysis by eq 5 yields the superimposed curves provided in Figure 8b and an effective diffusion coefficient of $(8.6 \pm 0.5) \times 10^{-7}$ cm^2/s irrespective of solution concentration. Note that this value is significantly higher (by almost 2 orders of magnitude) than that discerned for PEG_{400} in the swollen SEOS copolymer but is closer in magnitude to that measured[40] for PEG_{290} in water at 20 °C (D_{eff} = 3.7×10^{-6} cm^2/s) and determined[24] for PI in swollen SIS copolymers. This latter similarity may reflect homopolymer diffusion through a highly defective lamellar morphology, which is, in fact, observed[23] in the SIS/PI mesoblends and anticipated[11] for the AEG copolymer due to its molecular architecture.

The influence of C on S for PEG_{400} sorbed from water and ethanol solutions into the AEG copolymer for 100 h at 60 °C is presented in Figure 9 and closely resembles the analogous $S(C)$ trend exhibited by the SEOS copolymer in Figure 3. In both cases, the solubility of PEG_{400} imbibed from ethanol appears to reach a limiting value, whereas S increases monotonically when the carrier solvent is water. An important difference between the data shown in Figures 3 and 9 is that the solubility of PEG_{400} in the AEG copolymer is much less sensitive to solvent quality than that of PEG_{400} in the SEOS copolymer. Another intriguing feature of the data in these two figures is that the solubilities measured from both SEOS/PEG_{400} and AEG/PEG_{400} mesoblends prepared from PEG_{400}/water solutions are almost identical, which confirms our earlier conclusion that water is not a suitable carrier solvent for PEG sorption into a partially hydrophobic nanostructured matrix. The effect of M_{PEG} on the solubility of PEG sorbed from methanol (25% w/v solutions) at 23 °C in the swollen AEG copolymer is evident in Figure 10. As with the SEOS/PEG mesoblends (see Figure 4), an increase in M_{PEG} promotes a systematic reduction in S. Comparison of the two figures immediately reveals a striking difference in the dependence of S on M_{PEG}: S decreases nearly linearly with increasing M_{PEG} in Figure 4 but nonlinearly in Figure 10. Regressed scaling relationships of the form $S \sim M_{PEG}^{-\beta}$ are included for two values of β in Figure 10. The first ($\beta = 1/2$) corresponds to the scaling exponent deduced[24] from SIS/PI mesoblends but does not adequately fit the data as well as the second (β = 1). Thus, the dependence of S on M_{PEG} in AEG/PEG mesoblends is closer (but not identical) to that previously reported for SIS/PI mesoblends. This observation further supports our earlier contention based on effective diffusion coefficients that the defect-riddled SIS and

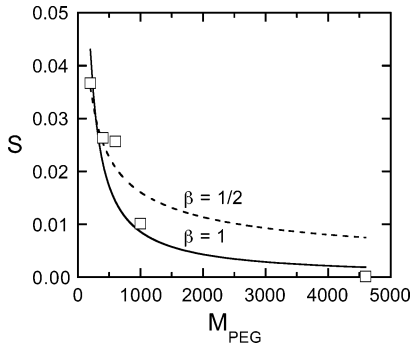

Figure 10. Dependence of PEG solubility in the AEG copolymer on PEG molecular weight (M_{PEG}) in 25% w/v methanol solutions at 23 °C. The lines are fits of the expression $S \sim M_{PEG}^{-\beta}$ to the data in which β is set equal to 1 (solid line) or $^1/_2$ (dashed line).

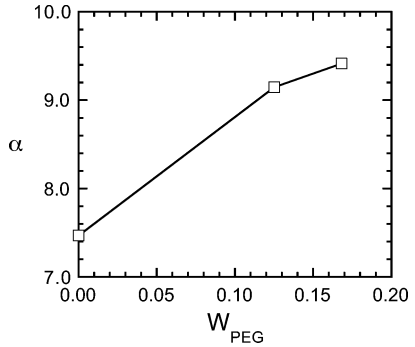

Figure 11. CO_2/H_2 selectivity (α) presented as a function of PEG concentration in AEG mesoblends immersed in 60% w/v PEG_{400} solutions in ethanol at 23 °C. The permeation tests used to calculate α have been performed at 23 °C and a transmembrane pressure of 6.8 atm. The solid line serves to connect the data.

AEG microdomains may provide similar nanostructured environments into which the relatively low-molar-mass homopolymers (PI or PEG) sorb from solution.

Since the nanostructure of the AEG copolymer is not expected[11] to possess the degree of long-range (periodic) order exhibited by the model SEOS copolymer and since the incorporation of PEG into the AEG copolymer is not anticipated to have a discernible effect on the thermal characteristics of the semicrystalline microdomains, we do not provide any morphological or thermal analyses of the AEG/PEG mesoblends produced here. Instead, we explore a property that has become closely associated[27,28] with the PEBAX copolymers, namely, CO_2 separation. Pure-gas permeabilities of CO_2 and H_2 have been measured from two AEG/PEG_{400} mesoblends after different exposure times to PEG_{400} (60% w/v in ethanol) at 23 °C. The CO_2/H_2 selectivity (α) calculated from eq 1 is displayed as a function of sorbed PEG (W_{PEG}) in Figure 11 and provides evidence that an increase in the PEG content of the AEG copolymer markedly improves the gas-separation efficacy of the mesoblend. To put these results in perspective, the maximum value of α obtained from the AEG/PEG mesoblend with 17 wt % sorbed PEG_{400} at ambient temperature and a transmembrane pressure of 6.8 atm is 9.4. Bondar et al.[27] report a CO_2/H_2 selectivity of 9.8 for the neat copolymer at 35 °C and a pressure of 10 atm. Even after taking into account the effect of gas pressure, the reason for the considerable difference in the measured value of α for the neat copolymer is not known, but incorporation of PEG certainly improves α in the present study. It

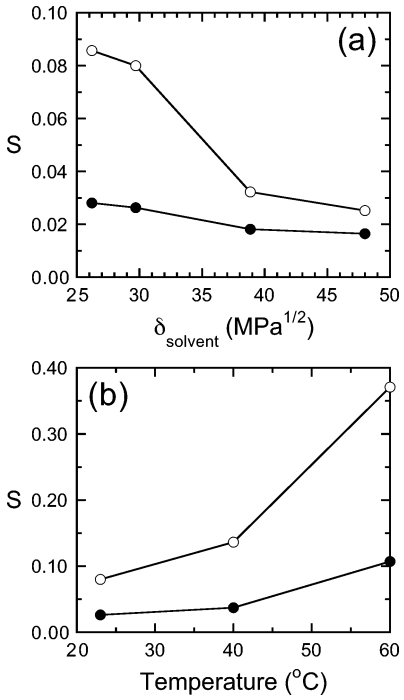

Figure 12. Variation of PEG_{400} solubility with (a) the solubility parameter (δ) of the carrier solvent and (b) temperature in the SEOS triblock copolymer (○) and the AEG multiblock copolymer (●) after an immersion time of 24 h in solutions containing 25% w/v PEG_{400}. The temperature in (a) is 23 °C for the AEG copolymer and 60 °C for the SEOS copolymer, and the solvent in (b) is methanol. The solid lines serve to connect the data.

should be noted that attempts to introduce PEG into the AEG copolymer by conventional codissolution/cocasting methods typically yield heterogeneous membranes due to the propensity of the AEG molecules to self-organize into highly interconnected nanoscale aggregates.[41]

Effects of Solvent Quality and Temperature on Both Mesoblend Series. The previous sections have examined the sorption kinetics and resultant property changes of PEG imbibed into two chemically dissimilar linear multiblock copolymers. Throughout these analyses, comparisons between the two mesoblend series have been made whenever possible. In this section, we present a direct comparison between the two series with regard to two environmental conditions: solvent quality and temperature. In Figure 12a, the solubility of PEG_{400} in the SEOS and AEG copolymers at 23 °C is provided as a function of solubility parameter (δ) for three pure solvents (water, ethanol, and methanol) and one miscible solvent mixture (50/50 v/v methanol/water) at a PEG_{400} concentration of 25% w/v. The dependence of S on increasing δ (solvent polarity) is slight in the case of the AEG copolymer but much more pronounced (especially at relatively low δ) for the SEOS copolymer. In highly polar solvents containing water, the solubility of PEG_{400} in each copolymer is surprisingly comparable. Recall, however, that the sorption temperature is below T_m in the SEOS copolymer. Figure 12b shows the dependence of PEG_{400} solubility on temperature in both copolymers immersed in methanol under similar sorption conditions. As the temperature is increased, S increases systematically in both mesoblend series. This can be generally attributed to accompanying increases in (i) the molecular mobility of PEG_{400} and (ii) the configurational entropy within the polyether micro-

domains of the copolymers. Once the EO crystals in the SEOS copolymer are melted at 60 °C, the solubility of PEG_{400} is observed to increase sharply, as anticipated from a comparison of Figures 3 and 4.

Conclusions

The uptake kinetics, morphological characteristics, and property changes associated with PEG sorption into two polyether-containing block copolymers to form nonequilibrium mesoblends have been investigated. The effective diffusion coefficient of PEG of a single molecular weight discerned from uptake kinetics is found to be independent of solvent quality and solution concentration, whereas the equilibrium solubility is sensitive to both considerations as well as PEG molecular weight. The mobility of PEG into the host microdomains of the copolymer matrix from solution is faster in the AEG multiblock copolymer than in the lamellar SEOS triblock copolymer due presumably to the lower degree of structural order (more diffusive pathways) in the former and the possibility of residual crystals (more diffusive obstacles) in the latter. The solubility of PEG sorbed from a polar organic solvent, on the other hand, is generally higher in the SEOS copolymer, which is less molecularly constrained than the multiblock copolymer and is capable of greater swelling. If the carrier is or contains water, the solubility of PEG in both copolymers is unexpectedly comparable. Incorporation of amorphous PEG into the SEOS copolymer can be spatially monitored by TEM, whereas the effect of imbibed PEG on the thermal characteristics of the resultant mesoblends is amenable to DSC analysis, which reveals the existence of a strong exothermic process suggestive of stress release at the polystyrene T_g in SEOS/PEG mesoblends containing a large fraction of sorbed PEG. Addition of PEG to the AEG copolymer likewise has a pronounced effect on gas transport properties. This work is part of a series that demonstrates the utility of mesoblends in (i) probing the thermodynamic and transport properties of homopolymer molecules in a swollen, molecularly confined environment and (ii) producing novel nonequilibrium materials with new properties in systematic fashion.

Acknowledgment. This work was supported by the U.S. Department of Energy under Contract DE-FG02-99ER14991.

References and Notes

(1) Paul, D. R.; Bucknall, C. B. In *Polymer Blends*; Paul, D. R., Bucknall, C. B., Eds.; Wiley: New York, 2000; Vol. 1, pp 1−14.
(2) Araki, T., Tran-Cong, Q., Shibayama, M., Eds.; *Structure and Properties of Multiphase Polymeric Materials*; Marcel-Dekker: New York, 1998.
(3) Utracki, L. A. *Polymer Alloys and Blends: Thermodynamics and Rheology*; Oxford University Press: New York, 1990.
(4) Krishnamoorthi, R., Vaia, R. A., Eds.; *Polymer Nanocomposites: Synthesis, Characterization and Modeling*; American Chemical Society: Washington, DC, 2002; Vol. 804.
(5) Bronstein, L. M. *Top. Curr. Chem.* **2003**, *226*, 55.
(6) Walls, H. J.; Riley, M. W.; Gupta, R. R.; Spontak, R. J.; Fedkiw, P. S.; Khan, S. A. *Adv. Funct. Mater.* **2003**, *13*, 710.
(7) Hamley, I. W. *The Physics of Block Copolymers*; Oxford University Press: Oxford, 1998.
(8) Bates, F. S.; Fredrickson, G. H. *Phys. Today* **1999**, *52*, 32.
(9) Leibler, L. *Macromolecules* **1980**, *13*, 1602.
(10) Stadler, R.; Auschra, C.; Beckmann, J.; Krappe, U.; Voigt-Martin, I.; Leibler, L. *Macromolecules* **1995**, *28*, 3080.
(11) Spontak, R. J.; Smith, S. D. *J. Polym. Sci., Part B: Polym. Phys.* **2001**, *39*, 947.
(12) Winey, K. I.; Thomas, E. L.; Fetters, L. J. *J. Chem. Phys.* **1991**, *95*, 9367. Winey, K. I.; Thomas, E. L.; Fetters, L. J. *Macromolecules* **1991**, *24*, 6182; **1992**, *25*, 2645. Urbas, A.; Sharp, R.; Fink, Y.; Thomas, E. L.; Xenidou, M.; Fetters, L. J. *Adv. Mater.* **2000**, *12*, 812.
(13) Tanaka, H.; Hashimoto, T. *Macromolecules* **1991**, *24*, 5713. Kimishima, K.; Hashimoto, T.; Han, C. D. *Macromolecules* **1995**, *28*, 3842. Bodycomb, J.; Yamaguchi, D.; Hashimoto, T. *Macromolecules* **2000**, *33*, 5187.
(14) Spontak, R. J.; Smith, S. D.; Ashraf, A. *Macromolecules* **1993**, *26*, 956.
(15) Schulz, M. F.; Bates, F. S.; Almdal, K.; Mortensen, K. *Phys. Rev. Lett.* **1994**, *73*, 86. Zhao, J.; Majumdar, B.; Schulz, M. F.; Bates, F. S.; Almdal, K.; Mortensen, K.; Hajduk, D. A.; Gruner, S. M. *Macromolecules* **1996**, *29*, 1204.
(16) Kane, L.; Satkowski, M. M.; Smith, S. D.; Spontak, R. J. *Macromolecules* **1996**, *29*, 8862. Spontak, R. J.; Fung, J. C.; Braunfeld, M. B.; Sedat, J. W.; Agard, D. A.; Kane, L.; Smith, S. D.; Satkowski, M. M.; Ashraf, A.; Hajduk, D. A.; Gruner, S. M. *Macromolecules* **1996**, *29*, 4494. Kane, L.; Norman, D. A.; White, S. A.; Matsen, M. W.; Satkowski, M. M.; Smith, S. D.; Spontak, R. J. *Macromol. Rapid Commun.* **2001**, *22*, 281.
(17) Abetz, V.; Goldacker, T. *Macromol. Rapid Commun.* **2000**, *21*, 16.
(18) Yamaguchi, D.; Shiratake, S.; Hashimoto, T. *Macromolecules* **2000**, *33*, 8258. Yamaguchi, D.; Hashimoto, T. *Macromolecules* **2001**, *34*, 6495. Yamaguchi, D.; Hasegawa, H.; Hashimoto, T. *Macromolecules* **2001**, *34*, 6506. Yamaguchi, D.; Takenaka, M.; Hasegawa, H.; Hashimoto, T. *Macromolecules* **2001**, *34*, 1707. Court, F.; Hashimoto, T. *Macromolecules* **2001**, *34*, 2536. Court, F.; Hashimoto, T. *Macromolecules* **2002**, *35*, 2566.
(19) Spontak, R. J.; Patel, N. P. In *Developments in Block Copolymer Science and Technology*; Hamley, I. W., Ed.; Wiley: New York, 2004; pp 159−212.
(20) Abetz, V. In *Encyclopedia of Polymer Science and Technology*, 3rd ed.; Kroschwitz, J. I., Ed.; Wiley: Hoboken, NJ, 2003; Vol. 1, pp 482−523.
(21) Zhulina, E. B.; Halperin, A. *Macromolecules* **1992**, *25*, 5730.
(22) King, M. R.; White, S. A.; Smith, S. D.; Spontak, R. J. *Langmuir* **1999**, *15*, 7886.
(23) Roberge, R. L.; Patel, N. P.; White, S. A.; Thongruang, W.; Smith, S. D.; Spontak, R. J. *Macromolecules* **2001**, *35*, 2268.
(24) Stevens, J. E.; Thongruang, W.; Patel, N. P.; Smith, S. D.; Spontak, R. J. *Macromolecules* **2003**, *36*, 3206.
(25) Simon, P. F. W.; Ulrich, R.; Spiess, H. W.; Wiesner, U. *Chem. Mater.* **2001**, *13*, 3464.
(26) Patel, N. P.; Miller, A. C.; Spontak, R. J. *Adv. Mater.* **2003**, *15*, 729.
(27) Bondar, V. I.; Freeman, B. D.; Pinnau, I. *J. Polym. Sci., Part B: Polym. Phys.* **1999**, *37*, 2463; **2000**, *38*, 2051.
(28) Kim, J.-H.; Seong, Y. H.; Lee, Y. M. *J. Membr. Sci.* **2001**, *190*, 179.
(29) Graham, T. *Philos. Mag.* **1866**, *32*, 401.
(30) Patel, N. P.; Spontak, R. J. *Macromolecules*, submitted for publication.
(31) Geng, H. Z.; Rosen, R.; Zheng, B.; Shimoda, H.; Fleming, L.; Liu, J.; Zhou, O. *Adv. Mater.* **2002**, *14*, 1387.
(32) Felder, R. M.; Huvard, G. S. In *Permeation, Diffusion and Sorption of Gases and Vapors*; Fava, R., Ed.; Academic Press: New York, 1978; Vol. 16C, p 315.
(33) Chen, H.-L.; Hsiao, S.-C.; Lin, T.-L.; Yamauchi, K.; Hasegawa, H.; Hashimoto, T. *Macromolecules* **2001**, *34*, 671.
(34) van Krevelen, D. W. *Properties of Polymers*; Elsevier Science B.V.: Amsterdam, 1997; pp 196−197, 572.
(35) Du, Y.; Xue, Y.; Frisch, H. L. In *Physical Properties of Polymers Handbook*; Mark, J. E., Ed.; AIP Press: New York, 1996; Chapter 16.
(36) Jonquières, A.; Clément, R.; Lochon, P. *Prog. Polym. Sci.* **2002**, *27*, 1803 and the references therein.
(37) Balik, C. M. *Macromolecules* **1996**, *29*, 3025.
(38) Patel, N. P. Ph.D. Dissertation, North Carolina State University, Raleigh, NC, 2004.
(39) Rohde-Liebenau, H. U. W. In *Polymer Data Handbook*; Mark, J. E., Ed.; Oxford University Press: New York, 1999; p 225.
(40) Yuan, Q. W. In *Polymer Data Handbook*; Mark, J. E., Ed.; Oxford University Press: New York, 1999; p 549.
(41) Borisov, O. V.; Halperin, A. *Macromolecules* **1996**, *29*, 2612; *Curr. Opin. Colloid Interface Sci.* **1998**, *3*, 415.

MA0356257